

Lipid spontaneous curvatures estimated from temperature-dependent changes in inverse hexagonal phase lattice parameters: the effects of metal cations

Marcus K. Dymond^{1*}, Richard J. Gillams², Duncan J. Parker², Jamie Burrell², Ana Labrador³, Tommy Nylander⁴, George S. Attard^{2*}

¹ Division of Chemistry, School of Pharmacy and Biomolecular Sciences, University of Brighton, Brighton, BN2 4GJ, UK

² Chemistry, Faculty of Natural & Environmental Sciences, University of Southampton, Southampton SO17 1BJ, UK

³ MAX IV Laboratory, Lund University, PO Box 118, SE-221 00, Lund, Sweden

⁴ Physical Chemistry, Lund University, PO Box 124, SE-221 00, Lund, Sweden

(*) Authors for correspondence: M.Dymond@brighton.ac.uk; gza@soton.ac.uk

Abstract

Recently we reported a method for estimating the spontaneous curvatures of lipids from temperature dependent changes in the lattice parameter of inverse hexagonal liquid crystal phases of binary lipid mixtures. This method makes use of 1,2-dioleoyl-*sn*-glycerol-3-phosphoethanolamine, (DOPE) as a host lipid, which preferentially forms an inverse hexagonal phase, to which a guest lipid of unknown spontaneous curvature is added. The lattice parameters of these binary lipid mixtures are determined by small angle X-ray diffraction at a range of temperatures and the spontaneous curvature of the guest lipid is determined from these data. Here we report the use of this method on a wide range of lipids under different ionic conditions. We demonstrate that our method provides spontaneous curvature values for DOPE, cholesterol and monoolein that are within the range of values reported in the literature. Anionic lipids 1,2-dioleoyl-*sn*-glycerol-3-phosphatidic acid (DOPA) and 1,2-dioleoyl-*sn*-glycerol-3-phosphoserine (DOPS) were found to exhibit spontaneous curvatures that depend on the concentration of divalent cations present in the mixtures. We show that the range of curvatures estimated experimentally for DOPA and DOPS can be explained by a series of equilibria arising from lipid-cation exchange reactions. Our data indicate a universal relationship between the spontaneous curvature of a lipid and the extent to which it affects the lattice parameter of the hexagonal phase of DOPE when it is part of a binary mixture. This universal relationship affords a rapid way of estimating the spontaneous curvatures of lipids that are expensive, only available in small amounts or are of limited chemical stability.

Introduction

Membrane curvature, curvature elastic stress and stored elastic energy are continuum properties dependent on the spontaneous curvature (c_0) of the lipids that comprise the bilayer. The spontaneous curvature is a material parameter, which corresponds to the curvature that an unconstrained monolayer of a lipid would adopt. This has been shown to play a critical role in the energetics of many of the lipid-protein interactions that occur in biological membranes^{1,2}. For example, curvature elastic stress, which arises from a system being forced to adopt a curvature that is different from c_0 , has been shown to modulate the activity of many membrane interacting proteins^{3,4} and drives the folding of other membrane bound proteins^{5,6}. These observations underpin the intrinsic curvature hypothesis, which postulates that cells regulate the composition of their biological membranes so that the net curvature elastic stress is under homeostatic control^{7–10}. This has led to the proposal that the antineoplastic activity of some types of amphiphilic compounds could be mediated by their effect on membrane curvature elastic stress^{11,12}. Lipids and lipid membranes are key to a range of biological processes and it therefore seems likely that membrane elastic properties – and hence the spontaneous curvatures of particular lipids are crucial for these processes. Thus determination of spontaneous curvature in relation to lipid composition could help in furthering our understanding of a range of pathologies, such as cancer¹³, Alzheimer's disease¹⁴ and obesity¹⁵, that involve lipid disorders.

Several theoretical models to describe the physics of biological membrane assembly have been proposed¹⁶. To investigate quantitatively whether or not particular biological processes are controlled or mediated by curvature elastic stress requires estimates of the spontaneous curvatures of the lipids that comprise the membrane. Typically, quantification of stored elastic energy uses small angle X-ray scattering (SAXS) to determine the spontaneous curvature of pure lipids. These methods involve studying lipids in the inverse hexagonal lyotropic liquid crystal phase (H_{II}) to determine the radius of curvature at the neutral plane of the lipid molecules at zero osmotic stress¹⁷, and this is defined as the spontaneous curvature of that lipid. It should be noted however that in practice many studies determine c_0 at the pivotal plane due to this being easier to achieve experimentally^{18–20} and in this manuscript we discuss all spontaneous curvatures as measured at the pivotal plane, unless otherwise noted. Lipids that do not ordinarily form H_{II} phases but which have negative spontaneous curvatures, albeit weak, can be induced to form H_{II} phases by the addition of long chain liquid hydrocarbons to relieve packing frustration. Binary lipid mixtures comprising a well-characterized H_{II} phase forming lipid (the host) and a guest lipid with unknown c_0 have been used to determine the spontaneous curvature of the guest lipid from changes in the lattice dimensions of

the phase as the concentration of guest molecules increases^{21–24}. Using this methodology and other related scattering techniques^{18,25} values for the spontaneous curvatures of a number of biologically relevant lipids have been reported. Although these experimental approaches to determining c_0 are well established^{26,27}, they involve lengthy experiments and require significant amounts of sample (typically > 100 mg). Consequently c_0 values have been documented for only a small number of lipids, mainly those that are most easily available, out of the rich diversity of lipid species that exist across the different domains of life. Even for the more common lipid species, there is a paucity of c_0 values in the presence of buffers, other ionic species or as a function of pH, but such data as are available show significant ionic effects. For example the spontaneous curvature of 1,2-dioleoyl-*sn*-glycero-3-phosphoserine (DOPS) is pH dependent²⁴ and the spontaneous curvature of 1,2-dioleoyl-*sn*-glycero-3-phosphatidic acid (DOPA) and lyso 1-oleoyl-2-hydroxy-*sn*-glycero-3-phosphatidic acid (OPA) are dependent on the surrounding divalent cation concentration^{28,29}.

In our recent work³⁰, in which we reported the formation of Fd3m inverse cubic phases in binary mixtures of oleic acid (OA) with 1,2-dioleoyl-*sn*-glycero-3-phosphoethanolamine (DOPE) or 1,2-dioleoyl-*sn*-glycero-3-phosphocholine (DOPC), we described a new way of estimating the spontaneous curvatures of lipids. This method made use of the temperature-induced lattice expansion of the H_{II} phase in a host-guest binary system using frustrated lipid mixtures. The advantages of our method of estimating c_0 are the speed with which data can be obtained and the relatively small amounts (< 1 mg) of lipids needed. However the extent to which the method is applicable to a wide range of lipid systems, and in particular to anionic lipids in the presence of divalent cations, is not known. Here we report data from a systematic application of our method to a selection of structurally diverse lipids, and to anionic lipids in media that contain divalent cations, and validate the range of applicability of our experimental methodology.

Experimental

DOPE, 1,2-phytanyl-*sn*-glycero-3-phosphoethanolamine (DiPhyPE), DOPS and DOPA were purchased from Avanti Polar Lipids (Alabama USA). *Trans*-retinoic acid (tRA), *trans*-retinal (tR) and *cis*-retinal (cR), calcium chloride, cholesterol (chol), monoolein (MO), magnesium chloride, chloroform and bis-tris were purchased from Sigma-Aldrich (UK). *Trans*, *trans*-2,4-decanedienal (DD) and *cis*-11-hexadecenal (HD) were purchased from Tokyo Chemical Industry UK Ltd. Ultrapure water of 18.2 mΩ conductivity (Barnstead Nanopure Diamond) was used for the preparation of all samples.

Lipid samples were analyzed in pure water and three different buffer solutions with varying concentrations of divalent cations [M^{2+}]; low divalent cation buffer (13 mM [M^{2+}]) (bis tris 150 mM, 10 mM $MgCl_2$ and 3 mM $CaCl_2$ at pH 7.0), medium divalent cation buffer (65 mM [M^{2+}]) (bis tris 150 mM, 50 mM $MgCl_2$ and 15 mM $CaCl_2$ at pH 7.0) and high divalent cation buffer (130 mM [M^{2+}]) (bis tris 150 mM, 100 mM $MgCl_2$ and 30 mM $CaCl_2$ at pH 7.0).

Preparation of lyotropic liquid crystal phases for X-ray measurements

Binary lipid samples were prepared by weighing dry quantities of DOPE (used as received), typically in the range of 50 to 100 mg, into 500 μ l microcentrifuge tubes. Smaller amounts of the secondary lipid (0.005 to 0.09 mole fractions) were prepared by adding microlitre volumes of lipid solutions, with known concentration, dissolved in HPLC grade chloroform. A further 200 μ l of chloroform was added to each sample and the dissolved lipids were mixed by vortexing before being dried overnight *in vacuo*.

The moisture content of the lipids was estimated to be $\leq 0.1\%$ w/w, leading to an uncertainty in the lipid composition of the mixtures of up to 2 %.

To prepare lyotropic liquid crystal preparations in excess of limiting hydration, 100 μ l of pure water or one of the buffer solutions was added to each dry lipid sample. All samples were mixed manually using a small spatula for several minutes prior to centrifugation at 17000 g (Heraeus Pico 17 Centrifuge) for 5 minutes. Manual mixing and centrifugation cycles were repeated three times before samples were incubated at 37°C for 2-3 days. Prior to data collection a further manual mixing and centrifugation cycle was carried out.

Small angle X-ray diffraction (SAXD) studies

SAXD studies were performed at the SAXS station I911-4 of the MAX IV Synchrotron, Lund, Sweden, extensive details of the experimental setup have been published previously^{30,31}. Figure S1 shows a representative SAXD image and Table S1 provides the lattice parameter data for all the samples we have analyzed.

Equilibrium association modelling

Equilibrium association models for anionic lipids and metal cations were simulated using COPASI 4.11 (Build 65), which is a simulator for biochemical networks. Reactions were modelled in a single compartment based on the following dissociation phenomena: $\text{MX}_2 \rightleftharpoons \text{M}^{2+} + 2\text{X}^-$ (dissociation of a divalent metal cation salt e.g. MgCl_2), $\text{NaX} \rightleftharpoons \text{Na}^+ + \text{X}^-$ (dissociation of a sodium salt e.g. NaCl), $\text{LNa} \rightleftharpoons \text{L}^- + \text{Na}^+$ (dissociation of sodium salt of anionic lipid), $\text{LM}^+ \rightleftharpoons \text{L}^- + \text{M}^{2+}$ and $\text{L}_2\text{M} \rightleftharpoons \text{L}^- + \text{LM}^+$ (dissociation of divalent cation salts of anionic lipids). Equilibrium association constants were calculated from the ratio of the association and dissociation reaction rates. Equilibrium concentrations of the lipid species LNa , L_2M , LM^+ and L^- were used to calculate the spontaneous curvatures of mixtures across the range of compositions that were investigated experimentally and these values were compared with the experimental data. Rate constants for the association and dissociation reactions were adjusted iteratively to minimize the variance between the calculated values of c_0 for all the mixtures studied and experimental values.

Results and discussion

Lattice parameters were calculated from SAXD data obtained from the H_{II} phases of a wide range of binary mixtures comprising DOPE and low concentrations (typically mole fractions ranging from 0.03 to 0.09) of a second guest lipid over the temperature range 27°C to 57°C. This method uses frustrated H_{II} phases and assumes that $c_{0\text{ mix}}$ and κ do not change with temperature, whereas in fact these parameters show weak temperature dependence^{21,32,33}. The method also assumes that κ of the host lipid is unaffected by the small amounts of guest lipid present in the mixtures³.

Spontaneous curvatures of guest lipids from host hexagonal phase dimensions

As we described previously³⁰, the change in lattice parameters of frustrated inverse hexagonal lyotropic phases observed by SAXD at different temperatures, can be used to obtain estimates of the spontaneous curvature of lipid mixtures ($c_{0\text{ mix}}$) and their component lipid species. The reasoning behind the method stems from the observation that the stored elastic energy in an inverse hexagonal cylinder of lipids increases as the principal curvature of the mixture deviates away from the spontaneous curvature of the lipid mixture ($c_{0\text{ mix}}$). The method is only applicable to composition ranges where there is a single lyotropic phase³⁰; a full derivation is provided in the Supporting Information.

In summary, for an ideal mixture of amphiphiles in the inverse hexagonal phase, the curvature $c_1 = 1/R_1$ (where R_1 is the radius of curvature measured from the center of the water filled hexagonal cylinder to the radius of the pivotal plane (R_p)²² i.e. the plane on which the area per lipid molecule is not changed upon applying a bending moment) is related to the spontaneous curvature of the mixture ($c_{0\text{ mix}}$) through the following expression,

$$\frac{1}{2} \left\{ \left(c_1^{(A)} \right)^2 - \left(c_1^{(B)} \right)^2 \right\} = c_{0\text{ mix}} \left\{ c_1^{(A)} - c_1^{(B)} \right\} + \frac{\Delta E_T}{\kappa} \quad (1)$$

where ΔE_T is the difference in stored elastic energy between the two temperatures and κ is the bilayer bending elastic modulus. A plot of $\frac{1}{2} \left\{ \left(c_1^{(A)} \right)^2 - \left(c_1^{(B)} \right)^2 \right\}$ against $\left\{ c_1^{(A)} - c_1^{(B)} \right\}$ for pairs of temperatures (A and B), gives a straight line, where the intercept of this line is equal to $\frac{\Delta E_T}{\kappa}$ and the slope is equal to the spontaneous curvature of the mixture, $c_{0\text{ mix}}$. Using the lattice parameters (L_p) of the binary lipid system data obtained by SAXD, $c_1^{(A)}$ and $c_1^{(B)}$ can be obtained since the inter-pore spacing d_l (equal to the lattice parameter for the H_{II} phase) at temperature A is related to $c_1^{(A)}$ as follows:

$$d_l^{(A)} = 2R_w^{(A)} + 2l^{(A)} \quad (2),$$

where $R_w^{(A)}$ is the radius of the water cylinder in the H_{II} phase and $l^{(A)}$ is the lipid length, both at temperature A, and

$$\frac{1}{c_1^{(A)}} = R_p^{(A)} = R_w^{(A)} + l_x^{(A)} = \left(\frac{d_l^{(A)}}{2} \right) - l_y^{(A)} \quad (3),$$

where

$$l^{(A)} = l_x^{(A)} + l_y^{(A)} \quad (4),$$

l_x is the distance from the pivotal plane to the edge of the water pore and l_y is the distance from R_p to the edge of the hydrocarbon cylinder as summarized in Figure S2. For the small changes in d_l , that occur at different temperatures, l_x or l_y is not expected to change significantly relative to R_w , hence R_p , at different temperatures, can be estimated from Eq. 3. Using independent structural data obtained for the inverse hexagonal phase of DOPE at 25°C (which is the closest published data

available to our starting temperature of 27°C), we estimate the value of l_y to be 0.835 nm, since $R_w = 2.11$ nm and $2l = 3.15$ nm³⁴ and for an unstressed hexagonal cylinder $R_0 \approx R_p$ and thus $c_0 = c_1$.

In our original estimate³⁰ we used the published value of c_0 for DOPE of -0.435 nm⁻¹³⁵ (measured at the pivotal plane) to determine l_y . This is at the extreme of reported values of the spontaneous curvature of DOPE in water (all measured at the pivotal plane unless otherwise stated), which range from -0.399 ± 0.005 nm⁻¹²¹ using tricosene measured at the neutral plane, -0.351 nm⁻¹²², -0.333 nm⁻¹²⁴ to -0.348 nm⁻¹ using tetradecane³⁶. Studies of the spontaneous curvature of DOPE in different buffers and salts yield c_0 values of -0.370 nm⁻¹ (25 mM Mes, 25 mM Tes at pH 7), -0.435 nm⁻¹ (25 mM Mes, 25 mM Tes at pH 7, 150 mM NaCl) and -0.456 nm⁻¹ (25 mM Mes, 25 mM Tes at pH 7, 150 mM NaCl, 25 mM CaCl₂) utilizing tetradecane²⁰. Investigation of the effect of temperature and calcium cations in the buffer HEPES (10 mM), utilizing tetradecane has shown that the range of c_0 for DOPE extends from -0.331 nm⁻¹ to -0.374 nm⁻¹³² at the pivotal plane. In this publication we use the value of c_0 for DOPE of -0.351 nm⁻¹ to determine l_y , which is intermediate in the range of DOPE c_0 values reported in the literature and the radius of the pivotal plane of inverse hexagonal cylinders of DOPE in water at 25°C. Therefore, whilst our method assumes c_0 is temperature independent, it effectively estimates the value of c_0 at the pivotal plane at 25°C, since it is parameterized at this temperature.

To estimate the spontaneous curvature of the guest lipid (j) in the DOPE host matrix, we assume ideal mixing of the components and that c_0 for a mixture ($c_{0\text{mix}}$) is the average of the c_0 values of its components, weighted by their mole fractions^{3,37}. Such that,

$$c_{0\text{mix}} = x c_{0\text{DOPE}} + (1 - x) c_{0j} \quad (5).$$

Where we have calculated c_{0j} in buffers other than water, we initially determine the c_0 of DOPE in that buffer using the method by fitting to Eq.1 to calculate c_{0j} . For all c_0 determinations, we conducted lattice parameter measurements at six different temperatures and in fitting the data to Eq. 1 we used all unique combinations of temperature pairs. For linear fits to Eq. 1, this approach yields R^2 values, approaching 1. The error in the calculation of $c_{0\text{mix}}$ therefore stems principally from error in the lattice parameter measurements which is dominated the accuracy of the measured lipid compositions (up to 2%, as discussed in the experimental section). We estimate that overall the precision of the method yields an error in c_{0j} of ± 5 to 10%, depending on the amount of incorporated lipid and apply an intermediate error value of ± 7.5 % to all c_{0j} values in Tables 1 and 2. The accuracy of our measurements i.e. the proximity of the $c_{0\text{mix}}$ values that emerge from our

calculations when compared to literature values is dependent on two key assumptions. The first is that the value of l_y and l_x does not change over the temperature range studied and the second is that l_y and l_x do not change over the composition range studied. As discussed these statements are not explicitly true but as we have noted previously l_x changes by less than 2% w.r.t. the changing radius of water cylinders in DOPC: DOG³⁰ inverse hexagonal phases and similar arguments have been presented for the dependence of DOPE phases with temperature³⁸ and composition^{20,22,24}.

The spontaneous curvatures of guest lipids in host DOPE inverse hexagonal phases

The lattice parameters for the inverse hexagonal phases used to obtain $c_{0\text{mix}}$ are provided in the Supporting Information, Table S1 and the c_{0j} values for the individual guest lipid are shown in Table 1. The first thing to note is that the coefficient of variance (standard deviation/ mean c_{0j} , expressed as a percentage) when calculated for the each lipid in Table 1 is typically in the range of 5 to 10%. This demonstrates that the previously estimated 5 to 10% error in c_{0j} is appropriate.

lipid j	Mf _j (in DOPE)	c_{0j} / nm^{-1}	c_{0j} error (\pm)	mean c_{0j}	s.d.
chol	0.05	-0.54	0.04	-0.47	0.05
	1	-0.46	0.03		
	3	-0.44	0.03		
	5	-0.45	0.03		
MO	1	-0.56	0.04	-0.54	0.03
	2	-0.55	0.04		
	3	-0.51	0.04		
diPhyPE	3	-0.67	0.05	-0.65	0.02
	6	-0.65	0.05		
	9	-0.63	0.05		
OA	2	-0.69	0.05	-0.71	0.03
	3	-0.70	0.05		
	4	-0.75	0.06		
cR	3	-1.08	0.08	-1.13	0.06
	6	-1.12	0.08		
	9	-1.20	0.09		
DD	5	-0.61	0.05	-0.63	0.05
	20	-0.58	0.04		
	30	-0.69	0.05		
HD	5	-0.52	0.04	-0.52	0.04
	20	-0.47	0.04		
	30	-0.56	0.04		

	3	-0.87	0.07		
tR	6	-1.20	0.09	-1.05	0.16
	9	-1.06	0.08		
tRA	6	-0.65	0.05	-0.63	0.04
	9	-0.60	0.05		

Table 1 spontaneous curvature data, $c_{0j} \pm 7.5\%$ error, for guest lipids in an inverse hexagonal DOPE host phase and excess water, where s.d. is the standard deviation of the mean c_{0j} and Mf_j is the mole fraction of lipid j in DOPE. Table S2 provides further details of $c_{0\text{ mix}}$ (i.e. the gradient determined from Eq. 1) and the individual R_0 and c_0 values for each sample analyzed. All c_{0j} determinations are at the pivotal plane.

Previous studies have shown that divalent cations have only minor effects on the structural properties of the inverse hexagonal phases of zwitterionic lipids such as DOPE²⁰, with c_0 measured at the pivotal plane increasing from -0.33 nm^{-1} in water to -0.35 nm^{-1} in 100 mM calcium chloride (10mM HEPES pH 7.2)³². Therefore to confirm the accuracy of the c_0 values that we estimate by our method we determined c_0 at the pivotal plane for DOPE in each of the buffers containing divalent cations, our results were in the range of -0.37 to -0.36 nm^{-1} for 13 mM, 65 mM and 130 mM $[M^{2+}]$ and in good agreement with the values in the literature.

The c_0 of cholesterol, at the pivotal plane, has been reported in the literature as -0.435 nm^{-1} in water³⁹, using tetradecane, and as $-0.49 \pm 0.01 \text{ nm}^{-1}$ ²¹ at the neutral plane and 35°C in water. From our data, the decrease in lattice parameter with increasing cholesterol content (Table S1) is consistent with cholesterol having a smaller radius of spontaneous curvature than DOPE. These lattice parameter data, in conjunction with our method, gives a range of c_0 values for cholesterol from -0.54 to -0.44 nm^{-1} with a mean c_0 for all mixture compositions of $-0.47 \pm 0.05 \text{ nm}^{-1}$, which is within the range of literature values. The spontaneous radius of curvature of MO has previously been reported as $-2.00 \pm 0.03 \text{ nm}$ ⁴⁰ at the pivotal plane, which corresponds to c_0 of -0.50 nm^{-1} , our method estimates c_0 to be a comparable value of $-0.54 \pm 0.03 \text{ nm}^{-1}$.

We also used our previous data for OA in DOPE, together with the c_0 for DOPE we use here, to re-estimate c_0 for OA monomers at the pivotal plane, which works out as $-0.71 \pm 0.03 \text{ nm}^{-1}$; as discussed previously³⁰ this is consistent with literature values⁴¹.

The good agreement between the c_0 values from our experiments and values reported in the literature for these very different lipids gives some confidence that our method of estimating c_0 is robust and applicable to a wide range of lipid structures. Moving away from well-characterized systems we were able to determine the spontaneous curvature of diPhyPE ($c_0 = -0.65 \pm 0.03 \text{ nm}^{-1}$). Given the wider cross-sectional area of the phytanyl chain, when compared to the oleoyl chain, this increase in spontaneous curvature relative to DOPE is consistent with expectations. Since OA has a significant negative spontaneous curvature we wondered whether long-chained aldehydes would also be type II lipids. From our SAXD data we estimate c_0 values for DD and HD to be $-0.63 \pm 0.05 \text{ nm}^{-1}$ and $-0.61 \pm 0.16 \text{ nm}^{-1}$ respectively, which are comparable to the c_0 value of OA. The type II characteristics of fatty acids and fatty aldehydes appear to be consistent across a diversity of molecular structures as shown by the c_0 values we estimated cR ($-1.13 \pm 0.06 \text{ nm}^{-1}$), tR ($-1.05 \pm 0.16 \text{ nm}^{-1}$) and tRA ($-0.63 \pm 0.04 \text{ nm}^{-1}$).

The spontaneous curvatures of anionic lipids in host DOPE inverse hexagonal phases

One of the most challenging issues in evaluating the role of stored elastic energy in mediating biological processes *in vivo* is disentangling the extent to which anionic lipid activation of some membrane proteins is driven by electrostatic forces rather than membrane stored elastic energy. This question is complicated to answer as the salts used in buffers for assaying enzyme activity might also effect on the spontaneous curvatures of anionic lipids. Literature values of the spontaneous curvature of DOPS highlight the sensitivity of c_0 to the ionic environment experienced by the anionic lipid. Detailed studies²⁴ show that at pH 7 the spontaneous curvature of DOPS is $+0.069 \text{ nm}^{-1}$, whilst at pH 2, where the anionic DOPS molecules are protonated, c_0 has been observed to be -0.435 nm^{-1} . Interestingly the presence of tetradecane appears to affect the degree of protonation of DOPS, driving it into flat lamellar sheets, rather than promoting the formation of curvature relaxed inverse hexagonal phases. This implies that the DOPS molecules are somewhat deprotonated in tetradecane containing systems²⁴. This can be explained as an effect of the tetradecane solubilised in the lipid layer and hence increasing the distance between the ionizable groups. This in turn reduces the repulsive electrostatic potential between the head groups and hence facilitates deprotonation.

Consequently the c_0 of DOPS is expected to depend on the anionic lipid concentration in binary mixtures with DOPE. At low DOPS mole fractions the average separation between anionic lipid molecules is sufficiently large that the contribution of electrostatic repulsion to spontaneous curvature will be principally driven by molecular shape. However as DOPS mole fraction increases electrostatic repulsion will play an increasingly significant role in determining c_0 . While there is some evidence of this trend in the literature⁴², the presence of metal cations can confound this effect. The presence of monovalent cations will act to screen headgroup charge⁴³ and divalent cations that associate strongly with the headgroups will promote the formation of DOPS dimers, bridged by the divalent metal, which are strongly type II lipids⁴⁴. These competing mechanisms, underpinned by association constants of different magnitudes, generic to anionic lipids, have been reported for systems like DOPA²⁰ and 1,2-dioleoyl-*sn*-glycero-3-phosphoglycerol (DOPG)⁴⁵. We therefore set out to determine how spontaneous curvature of DOPS and DOPA in DOPE inverse hexagonal phases changes in the presence of buffers with different concentrations of divalent cations [M^{2+}].

Table 2 shows that DOPS has a negative spontaneous curvature in buffers with different concentrations of divalent cations. However, unlike the case of zwitterionic or uncharged lipids, the c_0 of DOPS appears to change as a function of its concentration in the binary mixture, ranging from -0.50 nm⁻¹ to -0.14 nm⁻¹. This is indicated because the coefficient of variance (c_v) in some of these studies is in excess of the 10% tolerance previously identified. For example in DOPS 13 mM divalent cations the c_v is 19%, similarly in DOPA 65 mM divalent cations the c_v of DOPA is 23%.

lipid j	[M ²⁺]/ mM	Mf _j (in DOPE)	c_{0j} / nm ⁻¹	c_{0j} error (±)
DOPE	0	0	-0.37	0.03
	13	0	-0.37	0.03
	65	0	-0.36	0.03
	130	0	-0.36	0.03
DOPS	0	3	-0.41	0.03
		6	-0.35	0.03
		9	-0.26	0.02
DOPS	13	3	-0.41	0.03

		6	-0.22	0.02
		9	-0.14	0.01
DOPS	65	3	-0.43	0.03
		6	-0.41	0.03
		9	-0.49	0.04
DOPS	130	3	-0.42	0.03
		6	-0.43	0.03
		9	-0.42	0.03
DOPA	0	3	-0.43	0.03
		6	-0.42	0.03
		9	-0.34	0.03
DOPA	13	3	-0.42	0.03
		6	-0.36	0.03
		9	-0.31	0.02
DOPA	65	3	-0.42	0.03
		6	-0.58	0.04
		9	-0.68	0.05
DOPA	130	3	-0.45	0.03
		6	-0.54	0.04
		9	-0.54	0.04

Table 2 spontaneous curvature data, $c_{0j} \pm 7.5\%$ error, for guest lipids in an inverse hexagonal DOPE host phase and excess water. Mf_j is the mole fraction of lipid j in DOPE and $[M^{2+}]$ is the total divalent cation concentration. Table S3 provides further details of $c_{0\text{ mix}}$ (i.e. the gradient determined from Eq. 1) and the individual R_0 and c_0 values for each sample analyzed. All c_{0j} determinations are at the pivotal plane.

Figure 1A, shows that in the case of samples containing water or 13 mM $[M^{2+}]$ buffer, at limiting hydration, the estimated c_0 of DOPS initially decreases, and then increases as the amount of DOPS in DOPE increases, going through a minimum at ~ 3 mole %.

In the buffers with 65 mM and 130 mM divalent cations, Figure 1B, the c_0 of DOPS appears to decrease with increasing DOPS mole fraction.

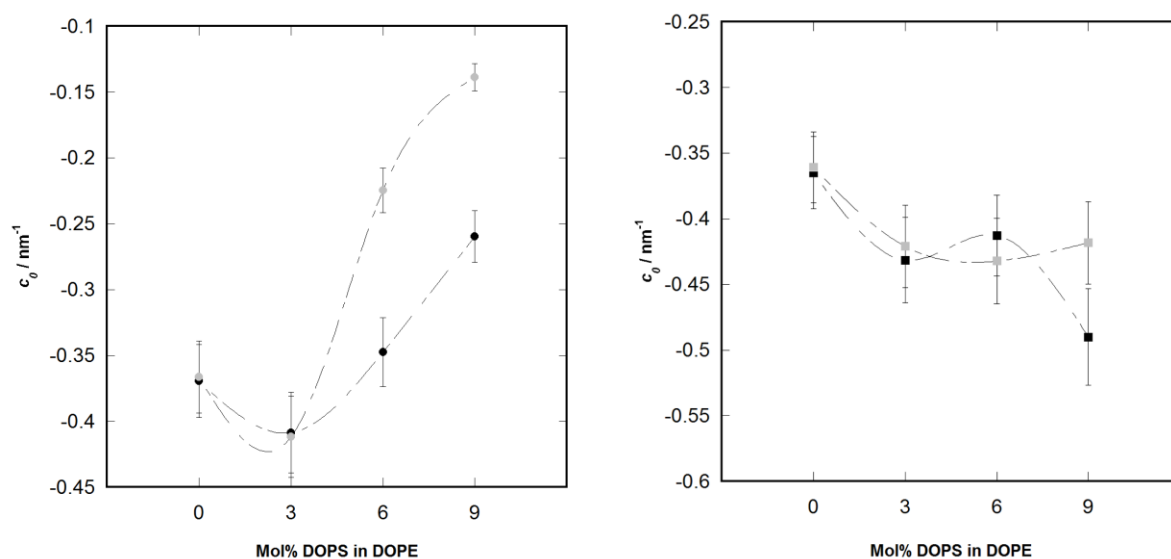


Figure 1A the compositional dependence of the c_0 , $\pm 7.5\%$ error, of DOPS in water (black circles) and 13 mM [M²⁺] buffer (grey circles); 1B the compositional dependence of the c_0 , $\pm 7.5\%$ error, of DOPS in 65 mM [M²⁺] buffer (black squares) and 130 mM [M²⁺] buffer (grey squares).

A similar set of trends is also observed for the dependence of the c_0 of DOPA in at different concentrations of divalent cations (Figures 2A and 2B).

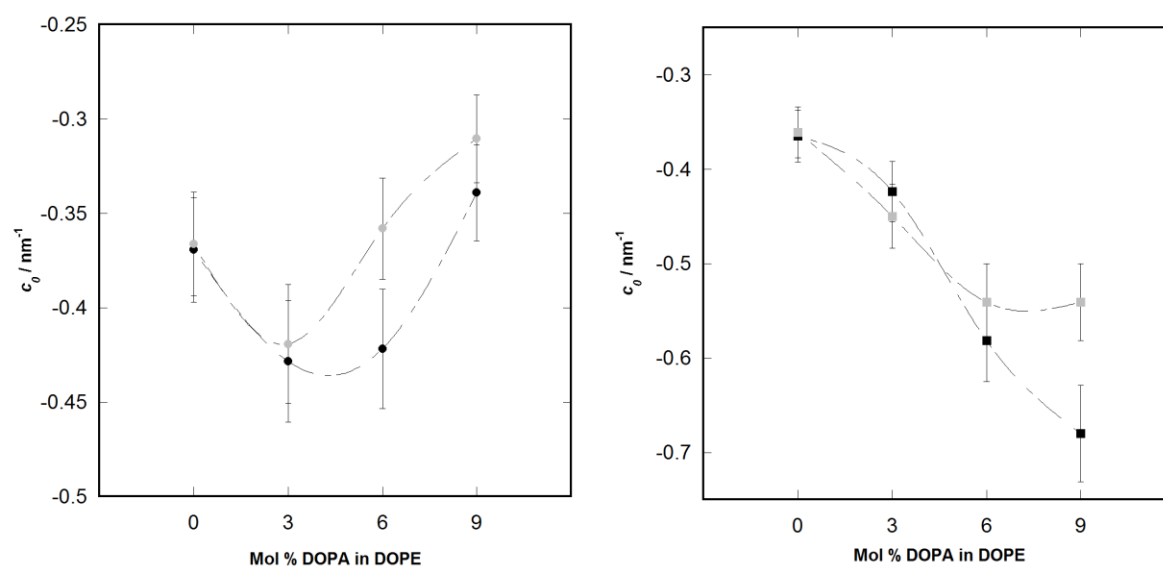


Figure 2A the compositional dependence of the c_0 , $\pm 7.5\%$ error, of DOPA in water (black circles) and 13 mM [M²⁺] buffer (grey circles); 2B the compositional dependence of the c_0 , $\pm 7.5\%$ error, of DOPA in 65 mM [M²⁺] buffer (black squares) and 130 mM [M²⁺] buffer (grey squares).

Taken together our estimates of c_0 for DOPS and DOPA suggest that the value of the spontaneous curvature of anionic lipids is highly dependent both on their concentration in a binary mixture and on the ionic strength of the buffer used to hydrate the H_{II} phase. This complex behavior may be rationalized by noting that as the amount of DOPS or DOPA in the mixture increases, the electrostatic repulsion between the anionic headgroups increases. This leads to an increase in the area occupied by the headgroups, therefore promoting a less negative interfacial curvature. The divalent cations Mg^{2+} and Ca^{2+} can also form bridges between the anionic lipids, which has an opposite effect and makes the headgroup area smaller and thus the curvature becomes more negative. Furthermore the sodium counterions of the DOPS and DOPA lipids could affect interfacial curvature through screening the anionic charge at the interface. This has been highlighted in a recent study, where the spontaneous curvature of DOPS in Ca^{2+} containing systems was found to be dependent on the concentration of monovalent cations⁴⁶. Thus, ultimately, the c_0 of an anionic lipid at a particular composition of the binary mixture and concentration of cations will be the sum of these processes. From this analysis it is reasonable to expect the spontaneous curvature to be dependent on the cation: lipid ratio. Thus care has to be taken before one can unambiguously correlate the c_0 of anionic lipids to biological activity. There are several reports in the literature that describe the effects of divalent cations on DOPA and it is well documented that divalent cations induce more negative curvature in these anionic systems. Recent work by Chen et al.³² shows that increasing the Ca^{2+} concentration in DOPE: DOPA mixtures (prepared in 10 mM HEPES at pH 7.2) decreases the measured c_0 of DOPA from -0.106 nm^{-1} in the absence of Ca^{2+} to -0.312 nm^{-1} in 100 mM Ca^{2+} . The c_0 values that emerge from our models are also negative, but assume more negative values of -0.4 nm^{-1} . The difference between these values might stem from differences in the amount of DOPE (3-9 wt% vs 10 wt%³²) or from different ratios of Ca^{2+} to DOPA between the two studies.

Since the method we use to determine the value of c_0 is an estimate it is important to question whether the different values of c_0 we calculate for DOPS and DOPA are genuine or artefacts of the estimate. To assess this we used our method to calculate c_0 from data in the literature detailing the temperature change of the lattice parameter of DOPE and DOPA mixtures, but obtained when using a ‘traditional’ method to calculate the spontaneous curvature. To achieve this we use the data of Chen et al.³², who reconstruct the electron density of the inverse hexagonal phase to determine the radius of the water cylinders (R_w) prior to determining c_0 at the pivotal plane for a number of different temperatures, DOPE: DOPA compositions and divalent cation concentrations. In Figures S3 to S5 we contrast the values reported by Chen et al.³² to the values obtained by our method but with their lattice parameter data; within error both techniques give the

same c_0 values as discussed section SI 1.2. This strongly suggests that the results shown in Figure 3A and 3B are not artefacts of the methodology.

To further investigate this we modelled the equilibrium association of DOPS and DOPA with cations and considered the resulting effects on the spontaneous curvature of DOPE: DOPA and DOPE: DOPS lipid mixtures.

Modelling the equilibrium association of anionic lipids with cations and the resultant spontaneous curvature

In order to assess quantitatively how the interactions between divalent cations and anionic lipids might account for the trends in c_0 that we observed experimentally, we set up a generic equilibrium model of the different species. The model accounts for the ion exchange between the sodium salt (LNa) of an anionic lipid and the salt (MX_2) of a divalent cation. The generic lipid species expected to occur at equilibrium, resulting from such an exchange process, would be: LNa, L^- , LM^+ , and L_2M as shown in Table 3 and Figure S6A. The total spontaneous curvature of the equilibrium mixture ($c_{0\text{ mix}}$) resulting from a particular set of equilibrium constants is calculated from the composition of the mixture by:

$$c_{0\text{ mix}} = (1 - w - x - y - z)c_{0\text{DOPE}} + wc_{0\text{LNa}} + xc_{0\text{L}_2\text{M}} + yc_{0\text{LM}^+} + zc_{0\text{L}^-} \quad (6)$$

We determined both the individual c_0 values and the equilibrium constants that gave rise to the concentrations w , x , y and z of LNa, L_2M , LM^+ and L^- in the hexagonal phase through iterative calculations selected for best fit to the experimental data. Table 3 shows the values of the equilibrium constants and c_0 for these mixtures.

Reaction	K_{eq} (L = DOPA)	K_{eq} (L = DOPS)	Species	c_0 (L = DOPA)	c_0 (L = DOPS)
$MX_2 \rightleftharpoons M^{2+} + 2X^-$	$1.0 \times 10^{12} \text{ M}^2$	$1.0 \times 10^{12} \text{ M}^2$	LNa	-0.33 (± 0.03)	-0.22 (± 0.02)
$NaX \rightleftharpoons Na^+ + X^-$	$1.0 \times 10^{12} \text{ M}$	$1.0 \times 10^{12} \text{ M}$	L^-	-0.28 (± 0.03)	-0.20 (± 0.02)
$L_2M \rightleftharpoons L^- + LM^+$	$1.0(\pm 0.7) \times 10^{-8} \text{ M}$	$1.0(\pm 0.7) \times 10^{-8} \text{ M}$	LM^+	-0.29 (± 0.03)	-0.15 (± 0.02)
$LM^+ \rightleftharpoons L^- + M^{2+}$	$1.67(\pm 0.20) \times 10^{-8} \text{ M}$	$2.0(\pm 0.2) \times 10^{-8} \text{ M}$	L_2M	-1.70 (± 0.12)	-1.30 (± 0.10)
$LNa \rightleftharpoons L^- + Na^+$	2 M	2.00 M	DOPE	-0.365	-0.365

Table 3 parameters used to fit the equilibria model of coexisting anionic lipid species to the experimentally determined mixture curvature values. LNa denotes the sodium salt of the anionic lipid (DOPA or DOPS), M^{2+} denotes a divalent cation (magnesium or calcium), X^- is an anion (chloride).

Figure 3 shows the fits of this model to the experimental data for DOPA and DOPS systems.

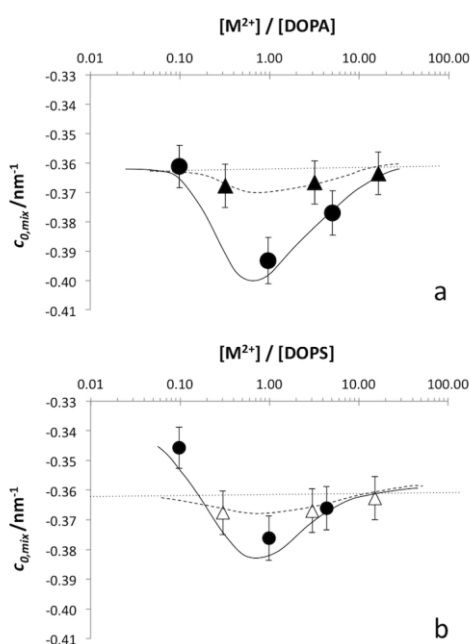


Figure 3 spontaneous curvatures of (A) DOPE:DOPA and (B) DOPE:DOPS mixtures as a function of the ratio of divalent cations to anionic lipids. Circles denote data for lipid concentration of 1.3×10^{-7} moles μL^{-1} ($Mf_j = 0.09$) and triangles for 4.0×10^{-8} moles μL^{-1} ($Mf_j = 0.03$). Curves through the data points are fits from the theoretical model of anionic lipid species equilibria. The horizontal dotted line denotes the value of c_{0j} for pure DOPE.

The data in Figure 3 show that our simple equilibrium model describes the change in the spontaneous curvature of DOPE mixtures containing DOPS and DOPA, at different divalent cation: anionic lipid ratios (Table 2). Figures S6B and S7 show how both the total spontaneous curvature and individual spontaneous curvatures of each of the components in the lipid mixture change with divalent cation concentration. This model highlights that increasing the relative concentration of divalent cations to anionic lipids leads to a maximum in c_0 for DOPA and, to a lesser extent, also for

DOPS. The few available relevant literature data for dissociation constants are also in reasonable agreement with the values obtained from our model. For example, literature values for the apparent association constant for the reaction $LNa \rightleftharpoons L^- + Na^+$ in vesicle systems are of the order of 2 M^{47} , where L is PS and measurements are made on a biological extract of bovine brain PS⁴⁴. Similarly, other data suggest that the dissociation constant of PS with Ca^{2+} is of the order of $1 \times 10^{-6} \text{ M}$. Both association constant values are within 2 orders of magnitude of the values that we determined by fitting the experimental data. This discrepancy is not surprising since in our model we don't distinguish between Mg^{2+} and Ca^{2+} and the dissociation equilibria in vesicle systems are unlikely to be the same as those in inverse hexagonal systems at limiting hydration.

As a final test we used a 'traditional' method to calculate the $c_{0\text{ mix}}$ values from the lattice parameter data we obtained for DOPE: DOPA and DOPE: DOPS mixtures but making use of the well-established relationship between limiting hydration fraction Φ_w , radius of the water cylinder and radius of the pivotal plane. We are able to do this because a number of literature studies have determined the limiting hydration value for DOPE: DOPS and DOPE: DOPA lipid mixtures in water and in the presence of divalent cations^{20,24,32}. This methodology is shown in the supporting information (SI 1.3), however we found that the trends in $c_{0\text{ mix}}$ that we report in Figure 3 were also apparent using this traditional approach, as best demonstrated by Figure S8.

Towards a phenomenological model for determining lipid spontaneous curvatures

We have determined a significant number of spontaneous curvature values for a range of structurally different lipids. These findings inspired us to establish a phenomenological approach that could be used to facilitate future spontaneous curvature estimates. This would be particularly advantageous when making spontaneous curvature estimates of expensive lipids or those available in limited amounts. Recognizing that the larger the difference between the spontaneous curvature of a guest lipid and that of DOPE, the larger the change in the lattice parameter of the H_{II} phase as a function of composition, we define the 'curvature power' of lipid j (χ_j) as:

$$\chi_j = (L_{p,PE(37)} - L_{p,j(37)}) / x_j \quad (7).$$

where $Lp_{j(37)}$ is the lattice parameter, at 37 °C, of lipid j , $Lp_{PE(37)}$ is the lattice parameter of DOPE and χ_j is the mole fraction of j . A plot of c_0 , estimated using our approach, against χ_j for all the lipids reported here is shown in Figure 4, where the data points for MO, OA and diPhyPE are highlighted.

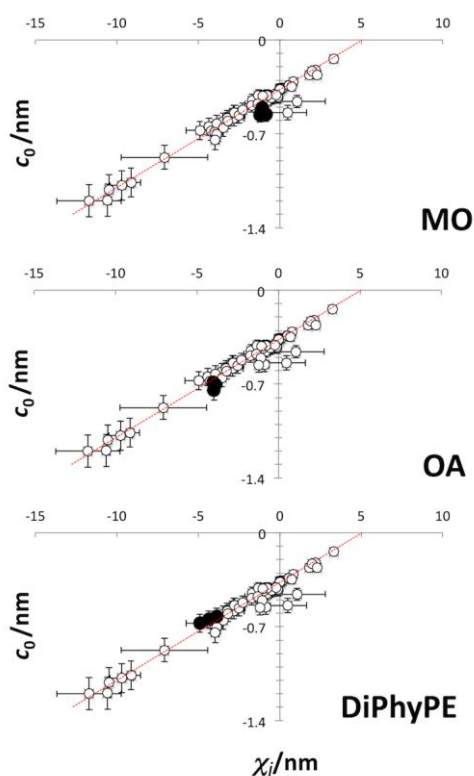


Figure 4 range of spontaneous curvatures determined from XRD data for the lipids MO, OA and DiPhyPE.

Figures S9 to S711 show the same data with the each of the other guest lipids highlighted. The universal curve can be fitted with the linear equation:

$$c_0 = 0.0731 \chi^2 - 0.3694 . \quad (8)$$

These plots allow us to construct a universal curve that can be used to estimate the c_{0j} value of a guest lipid directly from its effect on the lattice parameter of the inverse hexagonal phase of the host DOPE. Whilst this phenomenological approach may not have the same the accuracy in estimating c_0 as the method we developed, it does have the advantage of not requiring lattice parameter measurements to be made at different temperatures. This would speed up the generation of c_0 values, especially where the thermal stability of lipids is unclear, and eliminates one

of the assumptions in our model, namely that c_0 is invariant with temperature. We tested the predictive ability of this universal curve on literature X-ray diffraction data that we had not previously used in the development of this model. For example, Leikin et al.²² have determined the spontaneous curvature of 1,2-dioleoylglycerol (DOG) to be approximately -1.1 nm from DOPE: DOG mixtures and report the structural parameters of the inverse hexagonal phase determined by X-ray diffraction. Using Figure 4 as a calibration curve, in conjunction with the structural parameter data of Leikin et al.²² we determined the spontaneous radius of curvature of DOG to be -1.4 nm. The two values are in good agreement, suggesting that a phenomenological approach based on the ‘curvature power’ of a lipid might be a convenient and accessible way of estimating the c_0 values of lipids. Using this method we estimate the radius of spontaneous curvature of α -tocopherol to be -1.52 nm from the data of Bradford et al.⁴⁸, a tight curvature that is consistent with the observation that α -tocopherol promotes the formation of Fd3m phases⁴⁹. Similarly, we estimate the spontaneous curvature of elaidic acid to be -1.56 nm from the data of Funari et al.⁵⁰ indicating that it is also a Type II lipid.

Conclusions

In this paper we have validated our recently reported method for estimating the spontaneous curvatures of lipids from the temperature dependent changes in the lattice parameter of inverse hexagonal phases. Using the host lipid DOPE we determined the spontaneous curvatures of over 50 different lipid sample mixtures in around 1 week, including sample preparation, X-ray measurement and data analysis. It is apparent from the data we present here that our method is precise enough to give confident c_{0j} values to within a 5% to 10% error. The accuracy of our method will however always be below that of high resolution X-ray diffraction studies, but these investigations entail significant time to establish the true position of the pivotal or neutral surface. Furthermore, for most biophysical studies of lipid-protein interactions^{4,51} and computational models^{8,9,52,53} that are based on spontaneous curvature and stored elastic energy the accuracy of our approach is sufficient. We also note that in the case of DOPE, multiple estimates of c_0 exist in the literature, using a variety of X-ray diffraction methods (each of which quotes small errors in the value of c_0), there is a spread of c_0 values from -0.43 nm⁻¹ to -0.33 nm⁻¹ (\pm 13% of the mean).

We have here also presented a simple approach, based in the concept of the ‘curvature power’ of a lipid, which could be used to rapidly estimate the spontaneous curvature of guest lipids in DOPE inverse hexagonal phases. Whilst this phenomenological method is less accurate than our

temperature dependent method or other published methods¹⁷ for determining c_0 values, it is likely to be useful when a rough estimate of c_0 is required or when the availability and/ or stability of lipids is a limiting factor.

Our findings rely on a number of key assumptions i.e. that the spontaneous curvature is invariant with temperature and that ideal mixing exists between the host and guest lipids. It is interesting to consider at what point these assumptions break down and more importantly how this might be identified. In the case of ideal mixing it is anticipated that lateral domain formation will be one instance where Eq. 5 is not valid. In theory the best way to identify problems of this nature is to use different host molecules with the same guest to calculate the spontaneous curvature of the guest. If different values for the spontaneous curvature are being obtained with different hosts then it is an indication that the mixing might be non-ideal.

Supporting Information Available: [supplementary figures, mathematical derivation and lattice parameter measurements of binary lipid inverse hexagonal phases]. This material is available free of charge via the Internet at <http://pubs.acs.org>.

Competing Interests

The authors declare no competing interests.

Funding

DP and RJG gratefully acknowledge the award of studentships by Chemistry and by the University of Southampton Life Sciences Interfaces Forum respectively. MAX-lab IV is acknowledged for the beam time provided under proposals 20120231, 20120338 and 20130326. TN acknowledges financial support from the Swedish Research Council. MKD acknowledges start-up and capital funding from the School of Pharmacy and Biological Sciences, University of Brighton.

References

- (1) McMahon, H. T.; Gallop, J. L. Membrane Curvature and Mechanisms of Dynamic Cell Membrane Remodelling. *Nature* **2005**, *438* (7068), 590–596.
- (2) Ces, O.; Mulet, X. Physical Coupling between Lipids and Proteins: A Paradigm for Cellular Control. *Signal Transduct.* **2006**, *6* (2), 112–132.

- (3) Marsh, D. Lateral Pressure Profile, Spontaneous Curvature Frustration, and the Incorporation and Conformation of Proteins in Membranes. *Biophys. J.* **2007**, *93* (11), 3884–3899.
- (4) Attard, G. S.; Templer, R. H.; Smith, W. S.; Hunt, A. N.; Jackowski, S. Modulation of CTP:phosphocholine Cytidylyltransferase by Membrane Curvature Elastic Stress. *Proc. Natl. Acad. Sci. U. S. A.* **2000**, *97* (16), 9032–9036.
- (5) Booth, P. J.; Curnow, P. Folding Scene Investigation: Membrane Proteins. *Curr. Opin. Struct. Biol.* **2009**, *19* (1), 8–13.
- (6) Booth, P. J.; Riley, M. L.; Flitsch, S. L.; Templer, R. H.; Farooq, A.; Curran, a. R.; Chadborn, N.; Wright, P. Evidence That Bilayer Bending Rigidity Affects Membrane Protein Folding. *Biochemistry* **1997**, *36* (1), 197–203.
- (7) Gruner, S. M. Intrinsic Curvature Hypothesis for Biomembrane Lipid Composition: A Role for Nonbilayer Lipids. *Proc. Natl. Acad. Sci. U. S. A.* **1985**, *82* (11), 3665–3669.
- (8) Dymond, M. K.; Hague, C. V.; Postle, A. D.; Attard, G. S. An in Vivo Ratio Control Mechanism for Phospholipid Homeostasis: Evidence from Lipidomic Studies. *J. R. Soc. Interface* **2013**, *10* (80), 20120854.
- (9) Hague, C. V.; Postle, A. D.; Attard, G. S.; Dymond, M. K. Cell Cycle Dependent Changes in Membrane Stored Curvature Elastic Energy: Evidence from Lipidomic Studies. *Faraday Discuss.* **2013**, *161*, 481–497.
- (10) Dymond, M. K. Mammalian Phospholipid Homeostasis : Evidence That Membrane Curvature Elastic Stress Drives Homeoviscous Adaptation in Vivo. *J. R. Soc. Interface* **2016**, 20160228.
- (11) Dymond, M. K.; Attard, G. S. Cationic Type I Amphiphiles as Modulators of Membrane Curvature Elastic Stress in Vivo. *Langmuir* **2008**, *24* (20), 11743–11751.
- (12) Dymond, M. K.; Attard, G. S.; Postle, A. D. Testing the Hypothesis That Amphiphilic Antineoplastic Lipid Analogues Act through Reduction of Membrane Curvature Elastic Stress. *J. R. Soc. Interface* **2008**, *5* (28), 1371–1386.
- (13) Baenke, F.; Peck, B.; Miess, H.; Schulze, A. Hooked on Fat: The Role of Lipid Synthesis in Cancer Metabolism and Tumour Development. *Dis. Model. Mech.* **2013**, *6*, 1353–1363.
- (14) Paolo, G. Di; Kim, T. Linking Lipids to Alzheimer ' S Disease : Cholesterol and Beyond. *Nat Rev Neurosci* **2011**, *12* (5), 284–296.
- (15) Schwingshackl, L.; Hoffmann, G. Comparison of Effects of Long-Term Low-Fat vs High-Fat Diets on Blood Lipid Levels in Overweight or Obese Patients: A Systematic Review and Meta-Analysis. *J. Acad. Nutr. Diet.* **2013**, *113* (12), 1640–1661.
- (16) Deserno, M. Fluid Lipid Membranes: From Differential Geometry to Curvature Stresses. *Chem. Phys. Lipids* **2014**, *185*, 11–45.
- (17) Kozlov, M. M. Determination of Lipid Spontaneous Curvature from X-Ray Examinations of Inverted Hexagonal Phases. *Methods Mol. Biol.* **2007**, *400*, 355–366.
- (18) Fuller, N.; Rand, R. P. The Influence of Lysolipids on the Spontaneous Curvature and Bending Elasticity of Phospholipid Membranes. *Biophys. J.* **2001**, *81* (1), 243–254.
- (19) Szule, J. A.; Fuller, N. L.; Rand, R. P. The Effects of Acyl Chain Length and Saturation of Diacylglycerols and Phosphatidylcholines on Membrane Monolayer Curvature. *Biophys. J.* **2002**, *83* (2), 977–984.
- (20) Kooijman, E. E.; Chupin, V.; Fuller, N. L.; Kozlov, M. M.; De Kruijff, B.; Burger, K. N. J.; Rand, P. R. Spontaneous Curvature of Phosphatidic Acid and Lysophosphatidic Acid. *Biochemistry* **2005**, *44* (6), 2097–2102.

- (21) Kollmitzer, B.; Heftberger, P.; Rappolt, M.; Pabst, G. Monolayer Spontaneous Curvature of Raft-Forming Membrane Lipids. *Soft Matter* **2013**, 9 (45), 10877.
- (22) Leikin, S.; Kozlov, M.; Fuller, N.; Rand, R. Measured Effects of Diacylglycerol on Structural and Elastic Properties of Phospholipid Membranes. *Biophys. J.* **1996**, 71 (November), 2623–2632.
- (23) Epand, R. M.; Fuller, N.; Rand, R. P. Role of the Position of Unsaturation on the Phase Behavior and Intrinsic Curvature of Phosphatidylethanolamines. *Biophys. J.* **1996**, 71 (4), 1806–1810.
- (24) Fuller, N.; Benatti, C. R.; Rand, R. P. Curvature and Bending Constants for Phosphatidylserine-Containing Membranes. *Biophys. J.* **2003**, 85 (3), 1667–1774.
- (25) Winter, R.; Erbes, J.; Templer, R.; Seddon, J.; Syrykh, A.; Warrender, N. Inverse Bicontinuous Cubic Phases in Fatty Acid/phosphatidylcholine Mixtures: The Effects of Pressure and Lipid Composition. *Phys. Chem. Chem. Phys. PCCP* **1999**, 1, 887–893.
- (26) Pabst, G.; Kucerka, N.; Nieh, M.-P.; Rheinstädter, M. C.; Katsaras, J. Applications of Neutron and X-Ray Scattering to the Study of Biologically Relevant Model Membranes. *Chem. Phys. Lipids* **2010**, 163 (6), 460–479.
- (27) Tyler, A. I. I.; Law, R. V.; Seddon, J. M. X-Ray Diffraction of Lipid Model Membranes. *Methods Mol. Biol.* **2015**, 1232, 199–225.
- (28) Kooijman, E. E.; Chupin, V.; de Kruijff, B.; Burger, K. N. J. Modulation of Membrane Curvature by Phosphatidic Acid and Lysophosphatidic Acid. *Traffic* **2003**, 4 (3), 162–174.
- (29) Kooijman, E. E.; Carter, K. M.; van Laar, E. G.; Chupin, V.; Burger, K. N. J.; de Kruijff, B. What Makes the Bioactive Lipids Phosphatidic Acid and Lysophosphatidic Acid so Special? *Biochemistry* **2005**, 44 (51), 17007–17015.
- (30) Gillams, R. J.; Nylander, T.; Plivelic, T. S.; Dymond, M. K.; Attard, G. S. Formation of Inverse Topology Lyotropic Phases in Dioleoylphosphatidylcholine/oleic Acid and Dioleoylphosphatidylethanolamine/oleic Acid Binary Mixtures. *Langmuir* **2014**, 30 (12), 3337–3344.
- (31) Labrador, A.; Cerenius, Y.; Svensson, C.; Theodor, K.; Plivelic, T. The Yellow Mini-Hutch for SAXS Experiments at MAX IV Laboratory. *J. Phys. Conf. Ser.* **2013**, 425, 072019.
- (32) Chen, Y.-F.; Tsang, K.-Y.; Chang, W.-F.; Fan, Z. -a. Differential Dependencies on $[Ca^{2+}]$ and Temperature of the Monolayer Spontaneous Curvatures of DOPE, DOPA and Cardiolipin: Effects of Modulating the Strength of the Inter-Headgroup Repulsion. *Soft Matter* **2015**, 11 (20), 4041–4053.
- (33) Pan, J.; Tristram-Nagle, S.; Kucerka, N.; Nagle, J. F. Temperature Dependence of Structure, Bending Rigidity, and Bilayer Interactions of Dioleoylphosphatidylcholine Bilayers. *Biophys. J.* **2008**, 94 (1), 117–124.
- (34) Tate, M. W.; Gruner, S. M. Temperature Dependence of the Structural Dimensions of the Inverted Hexagonal (HII) Phase of Phosphatidylethanolamine-Containing Membranes. *Biochemistry* **1989**, 28 (10), 4245–4253.
- (35) Marsh, D. Intrinsic Curvature in Normal and Inverted Lipid Structures and in Membranes. *Biophys. J.* **1996**, 70 (5), 2248–2255.
- (36) Chen, Z.; Rand, R. P. Comparative Study of the Effects of Several N-Alkanes on Phospholipid Hexagonal Phases. *Biophys. J.* **1998**, 74 (2 Pt 1), 944–952.
- (37) Marsh, D. Elastic Curvature Constants of Lipid Monolayers and Bilayers. *Chem. Phys. Lipids* **2006**, 144 (2), 146–159.

- (38) Marsh, D. Pivotal Surfaces in Inverse Hexagonal and Cubic Phases of Phospholipids and Glycolipids. *Chem. Phys. Lipids* **2011**, *164* (3), 177–183.
- (39) Chen, Z.; Rand, R. P. The Influence of Cholesterol on Phospholipid Membrane Curvature and Bending Elasticity. *Biophys. J.* **1997**, *73* (1), 267–276.
- (40) Vacklin, H.; Khoo, B. J.; Madan, K. H.; Seddon, J. M.; Templer, R. H. Bending Elasticity of 1-Monoolein upon Relief of Packing Stress. *Langmuir* **2000**, *16* (10), 4741–4748.
- (41) Seddon, J. M.; Templer, R. H.; Warrender, N. A.; Huang, Z.; Cevc, G.; Marsh, D. Phosphatidylcholine-Fatty Acid Membranes: Effects of Headgroup Hydration on the Phase Behaviour and Structural Parameters of the Gel and Inverse Hexagonal (HII) Phases. *Biochim. Biophys. Acta* **1997**, *1327* (1), 131–147.
- (42) Kamal, M. M.; Mills, D.; Grzybek, M.; Howard, J. Measurement of the Membrane Curvature Preference of Phospholipids Reveals Only Weak Coupling between Lipid Shape and Leaflet Curvature. *Proc. Natl. Acad. Sci. U. S. A.* **2009**, *106* (52), 22245–22250.
- (43) Hauser, H.; Shipley, G. G. Interactions of Monovalent Cations with Phosphatidylserine Bilayer Membranes. *Biochemistry* **1983**, *22* (9), 2171–2178.
- (44) Hauser, H.; Darke, a; Phillips, M. C. Ion-Binding to Phospholipids. Interaction of Calcium with Phosphatidylserine. *Eur. J. Biochem.* **1976**, *62* (2), 335–344.
- (45) Alley, S. H.; Ces, O.; Barahona, M.; Templer, R. H. X-Ray Diffraction Measurement of the Monolayer Spontaneous Curvature of Dioleoylphosphatidylglycerol. *Chem. Phys. Lipids* **2008**, *154* (1), 64–67.
- (46) Simunovic, M.; Lee, K. Y. C.; Bassereau, P. Celebrating Soft Matter’s 10th Anniversary: Screening of the Calcium-Induced Spontaneous Curvature of Lipid Membranes. *Soft Matter* **2015**, *11*, 5030–5036.
- (47) Marsh, D. *Handbook of Lipid Bilayers*; CRC Press, 2013.
- (48) Bradford, A.; Atkinson, J.; Fuller, N.; Rand, R. P. The Effect of Vitamin E on the Structure of Membrane Lipid Assemblies. *J. Lipid Res.* **2003**, *44* (10), 1940–1945.
- (49) Bitan-Cherbakovsky, L.; Yuli-Amar, I.; Aserin, A.; Garti, N. Solubilization of Vitamin E into H(II) LLC Mesophase in the Presence and in the Absence of Vitamin C. *Langmuir* **2010**, *26* (5), 3648–3653.
- (50) Funari, S. S.; Barceló, F.; Escibá, P. V. Effects of Oleic Acid and Its Congeners, Elaidic and Stearic Acids, on the Structural Properties of Phosphatidylethanolamine Membranes. *J. Lipid Res.* **2003**, *44* (3), 567–575.
- (51) Tsaloglou, M.-N.; Attard, G. S.; Dymond, M. K. The Effect of Lipids on the Enzymatic Activity of 6-Phosphofructo-1-Kinase from *B. Stearothermophilus*. *Chem. Phys. Lipids* **2011**, *164* (8), 713–721.
- (52) Beard, J.; Attard, G. S.; Cheetham, M. J. Integrative Feedback and Robustness in a Lipid Biosynthetic Network. *J. R. Soc. Interface* **2008**, *5* (22), 533–543.
- (53) Dymond, M. K. Mammalian Phospholipid Homeostasis: Homeoviscous Adaptation Deconstructed by Lipidomic Data Driven Modelling. *Chem. Phys. Lipids* **2015**, *191*, 136–146.